Sea Ice Dynamics

Nan Chen, Zihong Xu

1 Introduction

Sea ice dynamics represent a complex system, with floe motion attributed to both underlying ocean flow fields and mutual interactions. These dynamics have significant implications for polar and global climates. Chen et al. (2021) introduced a Lagrangian data assimilation framework based on a discrete element model to describe floe dynamics, considering the impact of contact force and ocean flow field on sea ice floe trajectories. In this report, further adaptations will be explored, such as conducting data assimilation while excluding contact forces, adding dimensionality to the system, and implementing an Expectation-Maximization (EM) parameter estimation for floe thickness.

2 Ocean Field - Shallow Water Equation

One important aspect that governs the motion of ice floes is the underlying ocean flow. This is a variable that cannot be directly observed from satellite data, and thus also need to be recovered through data assimilation. In our experiment, the reference ocean flow field is followed by the shallow water equation represented by a set of hyperbolic partial differential equations.

$$\frac{\partial \mathbf{u}}{\partial t} + \epsilon^{-1}\mathbf{u}^{\perp} = -\epsilon^{-1}\nabla\eta \tag{1}$$

$$\frac{\partial \eta}{\partial t} + \epsilon^{-1}\delta\nabla\cdot\mathbf{u} = 0 \tag{2}$$

In this setup, $\mathbf{u}$ embeds a two-dimensional velocity field and η is the height function. The two non-dimensional numbers are $\epsilon = R_o$, Rossby number, and $\delta = \frac{R_o^2}{Fr^2}$, where Fr is the Froude number. Higher Rossby number typically means more dominant inertial forces compared to Coriolis force induced by earth rotation. The solution is typically given as the following expression. B is geostrophically balanced mode and $\pm$ is gravity modes.

$$\begin{pmatrix}\mathbf{u}_o(\mathbf{x},t)\\ \eta(\mathbf{x},t)\end{pmatrix} = \sum_{\mathbf{k}\in\mathbb{Z}^2,\zeta\in(B,\pm)} \hat{\mathbf{u}}_{\mathbf{k},\zeta}(t)\cdot e^{i\mathbf{k}\cdot\mathbf{x}}\mathbf{p}_{\mathbf{k},\zeta} \tag{3}$$

The Fourier coefficients then updates following a linear stochastic model. The $\phi_{\mathbf{k},\zeta}$ is the phase speed of different modes correspondingly.

$$d\hat{u}_{\mathbf{k},\zeta} = ((-d_{\mathbf{k},\zeta} + i\phi_{\mathbf{k},\zeta})\hat{u}_{\mathbf{k},\zeta} + f_{\mathbf{k},\zeta})dt + \sigma_{\mathbf{k},\zeta}dW_{\mathbf{k},\zeta} \tag{4}$$

$$\phi_{\mathbf{k},B} = 0 \tag{5}$$

$$\phi_{\mathbf{k},\pm} = \pm\epsilon^{-1}\sqrt{|\mathbf{k}|^2+1} \tag{6}$$

This system can be combined as vector representation. And after the fourier coefficient is reconstructed through iterations, the physical velocity field can be obtained through inverse fourier transform.

$$d\hat{\mathbf{u}}_o = (\mathbf{L}_{\mathbf{u}}\hat{\mathbf{u}}_o + \mathbf{F}_{\mathbf{u}})dt + \sum_{\mathbf{u}} d\mathbf{W}_{\mathbf{u}} \tag{7}$$

3 Physical System

In the realm of sea ice dynamics, both observable and unobservable variables exist, with the latter remaining inaccessible through available data sources. The goal of data assimilation is to derive these unobserved variables utilizing existing datasets. When it comes to sea ice dynamics, satellites can capture state variables like translational and angular displacements. However, recovering the driving velocities behind these state changes relies on the floe model, which outlines their mechanics. The floe dynamics model primarily involves contact forces, quadratic ocean drag forces, and random noises, culminating in the following comprehensive system.

$$d\mathbf{x}^l = \mathbf{v}^l \cdot dt + \sigma^l_{\mathbf{x}} \cdot d\mathbf{W}^l_{\mathbf{x}} \tag{8}$$

$$d\boldsymbol{\Omega}^l = \boldsymbol{\omega}^l \cdot dt + \sigma^l_{\boldsymbol{\Omega}} \cdot d\mathbf{W}^l_{\boldsymbol{\Omega}} \tag{9}$$

$$d\mathbf{v}^l = \frac{1}{m^l}(\sum_j (f^{lj}_n + f^{lj}_t) + \tilde{\alpha}^l(\mathbf{G}(\mathbf{x}^l)\hat{\mathbf{u}}_0 - \mathbf{v}^l)|\mathbf{G}(\mathbf{x}^l)\hat{\mathbf{u}}_0 - \mathbf{v}^l|) \cdot dt + \sigma^l_{\mathbf{v}} \cdot d\mathbf{W}^l_{\mathbf{v}} \tag{10}$$

$$d\boldsymbol{\omega}^l = \frac{1}{I^l}(\sum_j (r^l \cdot \mathbf{n}^{lj} \times \mathbf{f}^{lj}_{\mathbf{t}}) \cdot \hat{\mathbf{z}} + \tilde{\beta}^l(\nabla \times \hat{\mathbf{u}}_0/2 - \boldsymbol{\omega}^l \cdot \hat{\mathbf{z}})|\nabla \times \hat{\mathbf{u}}_0/2 - \boldsymbol{\omega}^l \cdot \hat{\mathbf{z}}|) \cdot dt + \sigma^l_{\boldsymbol{\omega}} \cdot d\mathbf{W}^l_{\boldsymbol{\omega}} \tag{11}$$

Though a bit complicated at first inspection, the main variables involved are observed sequences $\mathbf{x}^l$ and $\boldsymbol{\Omega}^l$, namely, translational and angular displacements, along with their unobserved velocity counterpart $\mathbf{v}^l$ and $\boldsymbol{\omega}^l$, and ocean flow field $\hat{\mathbf{u}}_0$. Henceforth, $\mathbf{X}$ will denote the two observed variables, and $\mathbf{Y}$ will include the three unobserved velocity components for all floes.

4 Discretization and Data Assimilation

The previous section has presented the comprehensive physical system of the floe model. In order to implement it, a discretized version is necessary, and this will be explicitly elaborated in this early section as reference for modifications in later experiments. By adopting the $\mathbf{X}$ and $\mathbf{Y}$ notation, the system of equations can be reduced to this general formulation.

$$d\mathbf{X}(t) = \mathbf{A}\mathbf{Y}(t)dt + \mathbf{B}d\mathbf{W}_{\mathbf{x}}(t) \tag{12}$$

$$d\mathbf{Y}(t) = [\mathbf{a}(\mathbf{X}(t)) + \mathbf{F}(\mathbf{X}(t), \mathbf{Y}(t))]dt + \mathbf{b}d\mathbf{W}_{\mathbf{Y}}(t) \tag{13}$$

Most of the vectors and matrices in this expression have simple structures, with the exception of $\mathbf{a}(\mathbf{X}(t))$ and $\mathbf{F}(\mathbf{X}(t), \mathbf{Y}(t))$, which include contact forces, quadratic drag forces, and torque imposed on the floes respectively. With this compact expression in hand, the discretization can be carried out effectively using Euler-Maruyama Scheme.

$$\mathbf{X}^{j+1} = \mathbf{X}^j + \mathbf{A}^j\mathbf{Y}^j\Delta t + \mathbf{B}\sqrt{\Delta t}\epsilon^j_{\mathbf{X}} \tag{14}$$

$$\mathbf{Y}^{j+1} = \mathbf{Y}^j + [\mathbf{a}(\mathbf{X}^j) + \mathbf{F}(\mathbf{X}^j, \mathbf{Y}^j)]\Delta t + \mathbf{b}\sqrt{\Delta t}\epsilon^j_{\mathbf{Y}} \tag{15}$$

Due to the nonlinear nature of $\mathbf{F}(\mathbf{X}^j, \mathbf{Y}^j)$, a conditional linearization approximation analogous to Taylor expansion is carried out to simplify the term.

$$\mathbf{F}(\mathbf{X}^j, \mathbf{Y}^j) = \mathbf{F}(\mathbf{X}^j, \boldsymbol{\mu}^j_f) + \mathbf{J}_{\mathbf{Y}}(\mathbf{X}^j, \boldsymbol{\mu}^j_f)(\mathbf{Y}^j - \boldsymbol{\mu}^j_f) + h.o.t \tag{16}$$

Then the $\mathbf{Y}$ term can be rewritten as the following.

$$\mathbf{Y}^{j+1} = \mathbf{Y}^j + [\mathbf{a}(\mathbf{X}^j) + \mathbf{F}(\mathbf{X}^j, \boldsymbol{\mu}^j_f) + \mathbf{J}_{\mathbf{Y}}(\mathbf{X}^j, \boldsymbol{\mu}^j_f)(\mathbf{Y}^j - \boldsymbol{\mu}^j_f)]\Delta t + \mathbf{b}\sqrt{\Delta t}\epsilon^j_{\mathbf{Y}} \tag{17}$$

$$= \mathbf{Y}^j + [\mathbf{a}(\mathbf{X}^j) + \mathbf{F}(\mathbf{X}^j, \boldsymbol{\mu}^j_f) - \mathbf{J}_{\mathbf{Y}}(\mathbf{X}^j, \boldsymbol{\mu}^j_f)\boldsymbol{\mu}^j_f + \mathbf{J}_{\mathbf{Y}}(\mathbf{X}^j, \boldsymbol{\mu}^j_f)\mathbf{Y}^j]\Delta t + \mathbf{b}\sqrt{\Delta t}\epsilon^j_{\mathbf{Y}} \tag{18}$$

Notice that the system dealt here after the linearization approximation matches exactly the conditional Gaussian model (Chen, 2020).

$$\mathbf{X}^{j+1} = \mathbf{X}^j + [\mathbf{A}^j_0 + \mathbf{A}^j_1\mathbf{Y}^j]\Delta t + \mathbf{B}\sqrt{\Delta t}\epsilon^j_{\mathbf{X}} \tag{19}$$

$$\mathbf{Y}^{j+1} = \mathbf{Y}^j + [\mathbf{a}^j_0 + \mathbf{a}^j_! \mathbf{Y}^j]\Delta t + \mathbf{b}\sqrt{\Delta t}\epsilon^j_{\mathbf{Y}} \tag{20}$$

Where the coefficients can be compared and the following expressions are derived.

$$\mathbf{A}_0 = 0 \tag{21}$$

$$\mathbf{A}_1 = \mathbf{A} \tag{22}$$

$$\mathbf{a}_0^j = \mathbf{a}^j + \mathbf{F}(\mathbf{X}^j, \boldsymbol{\mu}_\mathbf{f}^j) - \mathbf{J}_\mathbf{Y}(\mathbf{X}^j, \boldsymbol{\mu}_\mathbf{f}^j)\boldsymbol{\mu}_f^j \tag{23}$$

$$\mathbf{a}_1^j = \mathbf{J}_\mathbf{Y}(\mathbf{X}^j, \boldsymbol{\mu}_\mathbf{f}^j) \tag{24}$$

In the preliminary code, the general nonlinear optimal filter has the following form.

$$\boldsymbol{\mu}_f^{j+1} = \boldsymbol{\mu}_f^j + (\mathbf{a}_0 + \mathbf{a}_1\boldsymbol{\mu}_f^j) \cdot \Delta t + (\mathbf{R}_f^j\mathbf{A}^\dagger)(\mathbf{B}\mathbf{B}^\dagger)^{-1}(\mathbf{X}^{j+1} - \mathbf{X}^j - \mathbf{A}\boldsymbol{\mu}_f^j \cdot \Delta t) \tag{25}$$

$$\mathbf{R}_f^{j+1} = \mathbf{R}_f^j + (\mathbf{a}_1\mathbf{R}_f^j + \mathbf{R}_f^j\mathbf{a}_1^\dagger + \mathbf{b}\mathbf{b}^\dagger - (\mathbf{R}_f^j\mathbf{A}^\dagger)(\mathbf{B}\mathbf{B}^\dagger)^{-1}(\mathbf{A}\mathbf{R}_f^j)) \cdot \Delta t \tag{26}$$

In the following sections, multiple experiments will be carried out. Due to large reconstruction error that might be caused by the short period contact force in the data assimilation, the contact force will be removed in the data assimilation part. Although for simplicity, the contact force will also be removed in the model in early trials. Later, the contact force will be kept in true signal generation, namely, the floe model part, and provide piece-wise observations of short time period. Furthermore, the experiment will be dimensionalized to a more realistic setup. Finally, since neither the direct observation, nor the data assimilation will recover the floe thickness, an Expectation-Maximization parameter estimation scheme is required to estimate the parameters.

5 Elimination of Contact Forces

5.1 Elimination in Model and Data Assimilation

The collision between ice floes introduces significant errors in the model due to its short observation time. To address this issue, eliminate contact force is eliminated from the code. In this section, we discuss the removal of contact forces in both the ice floe model and the associated data assimilation step. For the model, normal and tangential forces are eliminated, as well as the v_{cx} and v_{cy} components. As a result, the ice floes eventually overlap with each other. In terms of data assimilation, we only need to focus on eliminating the contact force part in unobserved variables since all observed variables are contact-free.

The discretization of the contact-free ice floe model can be described as follows:

$$x^i = x^{i-1} + v_{ox}^{i-1} \cdot \Delta t + \sigma_x\sqrt{\Delta t}\epsilon_x^{i-1} \tag{27}$$

$$y^i = y^{i-1} + v_{oy}^{i-1} \cdot \Delta t + \sigma_y\sqrt{\Delta t}\epsilon_y^{i-1} \tag{28}$$

$$v_{ox}^i = v_{ox}^{i-1} + \frac{\alpha^l}{m}e^{i\mathbf{k}\cdot\mathbf{x}} \cdot (v_{field}^{i-1} - v_{ox}) \tag{29}$$

$$v_{ox}^i = v_{ox}^{i-1} + \frac{\alpha^l}{m}e^{i\mathbf{k}\cdot\mathbf{x}} \cdot (v_{field}^{i-1} - v_{ox}) \tag{30}$$

Additionally, there is a rotation force present. It is important to note that within the rotation force, there is a curl of the velocity field, which is equivalent to the velocity field multiplied by the eigenvectors of the Fourier modes and the wavenumber vector in spectral space. The eigenvectors of the modes here serve as a means to project the velocity field onto the eigenvector basis, thus isolating the contribution from different Fourier modes.

While performing data assimilation, contact force only takes place in the unobserved variables' equations. After the removal of contact force, both $\mathbf{A}_0$ and $\mathbf{a}_0^j$ are set to be zero, leaving only $\mathbf{A}_1 = \mathbf{A}$, the observation matrix, and $\mathbf{a}_1^j$, the Jacobian matrix.

$$\mathbf{A}_0 = [0] \tag{31}$$

$$\mathbf{A}_1 = \mathbf{A} \tag{32}$$

$$\mathbf{a}_0^j = \mathbf{a}^j + \mathbf{F}(\mathbf{X}^j, \boldsymbol{\mu}_\mathbf{f}^j) - \mathbf{J}_\mathbf{Y}(\mathbf{X}^j, \boldsymbol{\mu}_\mathbf{f}^j)\boldsymbol{\mu}_f^j = [0] \tag{33}$$

$$\mathbf{a}_1^j = \mathbf{J}_\mathbf{Y}(\mathbf{X}^j, \boldsymbol{\mu}_\mathbf{f}^j) \tag{34}$$

The filtering iteration then reduces to the following expression.

$$\boldsymbol{\mu}_f^{j+1} = \boldsymbol{\mu}_f^j + (\mathbf{a}_1 \boldsymbol{\mu}_f^j) \cdot \Delta t + (\mathbf{R}_f^j \mathbf{A}^\dagger)(\mathbf{B}\mathbf{B}^\dagger)^{-1}(\mathbf{X}^{j+1} - \mathbf{X}^j - \mathbf{A}\boldsymbol{\mu}_f^j \cdot \Delta t) \tag{35}$$

$$\mathbf{R}_f^{j+1} = \mathbf{R}_f^j + (\mathbf{a}_1 \mathbf{R}_f^j + \mathbf{R}_f^j \mathbf{a}_1^\dagger + \mathbf{b}\mathbf{b}^\dagger - (\mathbf{R}_f^j \mathbf{A}^\dagger)(\mathbf{B}\mathbf{B}^\dagger)^{-1}(\mathbf{A}\mathbf{R}_f^j)) \cdot \Delta t \tag{36}$$

6 Dimensionalization

While the currently presented experiments have been conducted in a non-dimensional context, it is essential to translate these findings into real-world scenarios by dimensionalizing the setup. This can be achieved by introducing real-world parameters such as length, mass, and time scales, as well as the actual values of the dimensionless numbers. By implementing these parameters, the model becomes more representative of the actual behavior of sea ice floes and their corresponding dynamics. Generally, there are two ways of dimensionalizing the system, one being dimensionalizing at the end of conversion, and the other dimensionalizing each variable during the process. However, here a mixed methodology is being applied here, where only the final ocean velocity field is dimensionalized since this will be a fixed quantity. For the floe model, we will have certain parameters to be also dimensionalized.

6.1 Generating Initial Floes

While generating the initial floes for the process, the radius, position, and thickness of the floes need to be dimensionalized. For the lateral length scale, all the parameters should be stretched by a factor of $\frac{50}{2\pi}$, and that includes the domain and the floe radius. For the domain, the 2π by 2π region is expanded to $50km$ by $50km$ domain. The radii for 36 floes are generated following a power law distribution $p(r) = \frac{ak^a}{r^{a+1}}$ with $k = 1.5, a = 1$ ranging from $\frac{2\pi}{25}$ to $\frac{2\pi}{10}$. The non-dimensional vector of radii generated is scaled up by $\frac{50}{2\pi}$.

$$radius_D = radius_{ND} \cdot \frac{50}{2\pi} \tag{37}$$

Empirically, the thickness of the floes should be converted to km from m and no scaling is needed.

$$thickness_D = thickness_{ND} \cdot \frac{1}{1000} \tag{38}$$

6.2 Shallow Water Equation

Besides the dimensional variables inherited from the initial floe generation, no further modification is needed for generating the underlying ocean flow field other than changing the period of the fourier basis from 2π to $50km$ and scale the final velocity field in the physical space by $\frac{50}{2\pi}$.

6.3 Floe Model

Floe model is the relatively complicated one to dimensionalize compared to the previous two. First of all, the ocean and ice density are all assumed to be $10^{12} kg/km^3$, where the non-dimensional value is 1. Then the random noise in the tracer equation, namely, position update equation should be scaled up.

$$\sigma_x^D = \frac{50}{2\pi} \sigma_x^{ND} \tag{39}$$

While standard dimensionalization of floe velocity and fourier basis function need to be scaled up by a factor of $\frac{50}{2\pi}$, the important thing is to balance the two non-dimensional coefficients $\frac{\alpha^l}{m}$ and $\frac{\beta^l}{I}$. Below a comparison for the non-dimensional coefficients and the dimensionalized ones is given in terms of their final expression, where i subscript stands for non-dimensional initial system, and f stands for the final system with dimensionalized variables. Since the value of ocean and ice density are taken to be the same in this

case, they will all be denoted by the same ρ_i and ρ_f.

$$d_o = 1, \rho_i = 1, h_i = 1, \rho_f = 10^{12}, h_f = \frac{h_i}{10^3} \tag{40}$$

$$\frac{\alpha_i^l}{m_i} = \frac{d_o \rho_i \pi r_i^2}{\rho_i \pi r_i^2 h_i} = \frac{d_o}{h_i} = 1 \tag{41}$$

$$\frac{\alpha_f^l}{m_f} = \frac{d_o \rho_f \pi r_f^2}{\rho_f \pi r_f^2 h_f} = \frac{d_o}{h_f} = 10^3 \tag{42}$$

$$\tag{43}$$

There are two ways to address this issue. The first is that a 10^{-3} factor can be added to the α_f^l expression, making it $\alpha_f^l = d_o \rho_f \pi r_f^2 \cdot 10^{-3}$. The other way is to add the thickness variable back into the α expression, and the ratio automatically turns into d_o itself which is already non-dimensionalized and requires no further modification. Similar analysis is applied to the angular velocity case. Same solutions could be applied.

$$\frac{\beta_i^l}{m_i} = \frac{d_o \rho_f \pi r_f^2 r_f^2}{\rho_i \pi r_i^2 h_i r_i^2} = \frac{d_o}{h_i} = 1 \tag{44}$$

$$\frac{\beta_i^l}{m_i} = \frac{d_o \rho_f \pi r_f^2 r_f^2}{\rho_f \pi r_f^2 h_f r_f^2} = \frac{d_o}{h_f} = 10^3 \tag{45}$$

$$\tag{46}$$

Everything left in the floe model and data assimilation part is simply changing every 2π concerned with the region size to $50km$ and a purely scaled-up version of the dynamics is achieved.

6.4 Result

After the dimensionalization process discussed above, the resulting system is the exact same amplification as the original non-dimensional system. The most important thing to check is that the first and final positions of the floes are the same. The velocity time series plots also serve as proof of reasonable dimensionalization of the system.

7 EM Parameterization

1. compare 2. parameterization 3. converge to Jeff's model

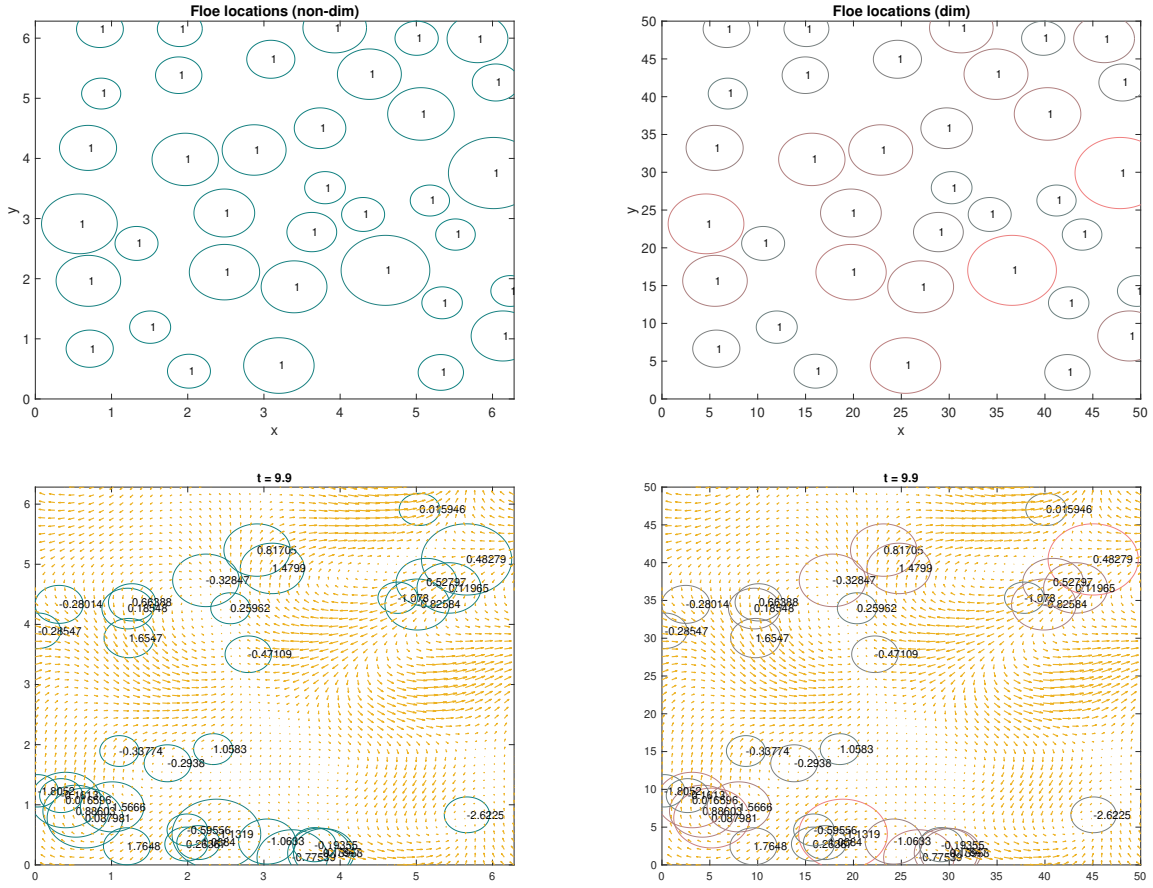

Figure 1: Comparison of floes initial and final positions before (left) and after (right) dimensionalization

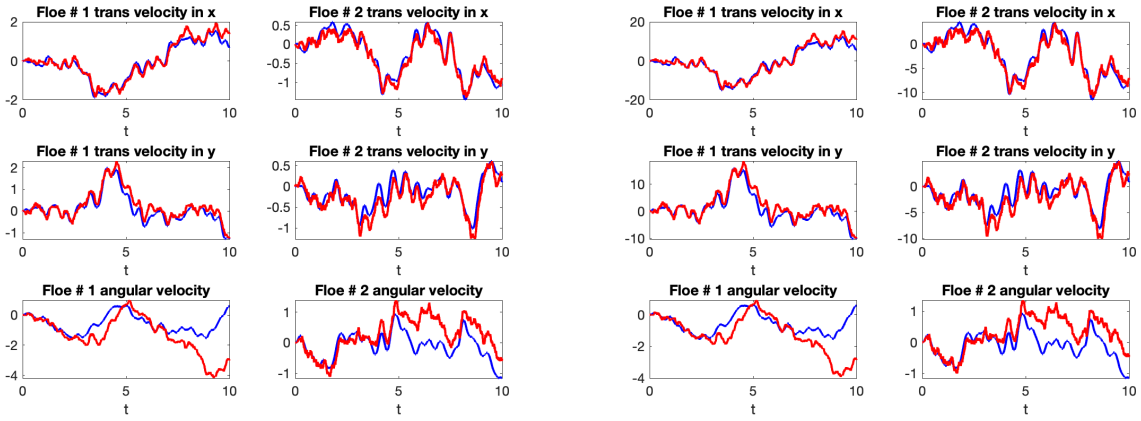

Figure 2: Comparison of velocity and angular velocity time series before (left) and after (right) dimensionalization, same pattern with different scales